

Decoding the mechanism of the mechanical transfer of a GaN-based heterostructure via an h-BN release layer in a device configuration

Gaoxue Wang, D. Z. Yang, Z. Y. Zhang, M. S. Si, Desheng Xue, Haiying He, and Ravindra Pandey

Citation: *Applied Physics Letters* **105**, 121605 (2014); doi: 10.1063/1.4896506

View online: <http://dx.doi.org/10.1063/1.4896506>

View Table of Contents: <http://scitation.aip.org/content/aip/journal/apl/105/12?ver=pdfcov>

Published by the *AIP Publishing*

Articles you may be interested in

[Single crystalline Sc₂O₃/Y₂O₃ heterostructures as novel engineered buffer approach for GaN integration on Si \(111\)](#)

J. Appl. Phys. **108**, 063502 (2010); 10.1063/1.3485830

[Effects of ZnO buffer layers on the fabrication of GaN films using pulsed laser deposition](#)

J. Appl. Phys. **101**, 093519 (2007); 10.1063/1.2730573

[Growth of high crystalline quality semi-insulating GaN layers for high electron mobility transistor applications](#)

J. Appl. Phys. **100**, 033501 (2006); 10.1063/1.2221520

[Growth stresses and cracking in GaN films on \(111\) Si grown by metal-organic chemical-vapor deposition. I. AlN buffer layers](#)

J. Appl. Phys. **98**, 023514 (2005); 10.1063/1.1978991

[Enhancement of breakdown voltage by AlN buffer layer thickness in Al Ga N/Ga N high-electron-mobility transistors on 4 in. diameter silicon](#)

Appl. Phys. Lett. **86**, 123503 (2005); 10.1063/1.1879091

The advertisement features a blue background with a film strip on the left side. The text is centered and reads: 'Not all AFMs are created equal' in orange, 'Asylum Research Cypher™ AFMs' in white, and 'There's no other AFM like Cypher' in orange. At the bottom, the website 'www.AsylumResearch.com/NoOtherAFMLikeIt' is listed in white, and the Oxford Instruments logo is in the bottom right corner with the tagline 'The Business of Science®'.

Decoding the mechanism of the mechanical transfer of a GaN-based heterostructure via an *h*-BN release layer in a device configuration

Gaoxue Wang,^{1,2} D. Z. Yang,¹ Z. Y. Zhang,¹ M. S. Si,^{1,a)} Desheng Xue,¹ Haiying He,^{3,b)} and Ravindra Pandey²

¹Key Laboratory for Magnetism and Magnetic Materials of the Ministry of Education, Lanzhou University, Lanzhou 730000, China

²Department of Physics, Michigan Technological University, Houghton, Michigan 49931, USA

³Department of Physics and Astronomy, Valparaiso University, Valparaiso, Indiana 46383, USA

(Received 31 March 2014; accepted 12 September 2014; published online 23 September 2014)

Mechanical transfer of GaN-based heterostructures using *h*-BN as the release layer [Y. Kobayashi, K. Kumakura, T. Akasaka, and T. Makimoto, *Nature* **484**, 223 (2012)] has promising applications for the next-generation optoelectronic devices. We investigate such transfer mechanism by mapping out the interlayer sliding energy landscape at each interface of a model heterostructure composed of GaN/BN/substrate together with the reference case of BN/BN interlayer sliding. The calculated results based on density functional theory find a nearly free sliding path for BN/BN, while a slightly higher energy barrier is predicted for hetero-interfaces of strained GaN/BN and BN/graphene substrate. The unstrained GaN/BN interface facilitates an easier peel-off of GaN from the BN layer. Thus, the sliding mechanism, which can also be described by the registry index model, shows dominance of the electrostatic interaction terms associated with the constituent layers of the system, though the van der Waals interaction term seems to determine the equilibrium interlayer distance for the systems considered. © 2014 AIP Publishing LLC.

[<http://dx.doi.org/10.1063/1.4896506>]

Nitride-based semiconducting materials have attracted a great amount of attention in the past few decades owing to their applications in the electronic and optoelectronic devices.¹ Among the nitrides, GaN is by far the most vastly studied owing to the virtues that it can enable full-color displays;² Mg-doped GaN could give rise to a broad blue luminescence band.³ However, most of the high quality GaN-based devices are only grown on the sapphire substrates, which substantially block the route to the large-scale fabrication of GaN-based devices. This is due to the fact that the sapphire substrates, in general, have a very poor thermal conductivity, and thus the accumulated heat in devices cannot be dissipated into the environment in a timely manner.⁴ This limitation can be addressed by mechanically releasing the high quality GaN-based devices from the sapphire substrate, and transferring them to another appropriate substrate.⁵

A recent work has shown that the multi-layer hexagonal (*h*)-BN can be successfully used as a release layer for the separation of the GaN-based devices from the sapphire substrate.⁶ The unsettled questions, however, are—how *h*-BN acts as a release layer and why the separation does not occur at the interface of *h*-BN and the device or *h*-BN and the substrate. In order to address such questions, we have performed a theoretical study based on density functional theory (DFT) and the registry index model. In this study, we employ the slab model to mimic the transfer process for the heterostructures, in which the GaN monolayer is deposited on the substrate via the *h*-BN release layer (Fig. 1). Calculations are performed to map out the sliding energy landscape for the interfaces including GaN/BN, BN/substrate, and BN/BN.

We note that a nearly free sliding path for the BN bilayer was previously reported.^{7,8}

The generalized gradient approximation (GGA) of the revised Perdew–Burke–Ernzerhof (revPBE)⁹ and the Perdew–Burke–Ernzerhof with the van der Waals (vdW) correction terms (vdW + PBE)¹⁰ were employed using the SIESTA code.¹¹ The plane wave cutoff energy of 400 Ry and a vacuum distance of 25 Å were used. The (11 × 11 × 1) Monkhorst-Pack *k*-grid was used for the geometry optimization. The total energy is converged to 10^{−6} eV. All atoms are allowed to relax and the convergence force is smaller than 0.01 eV/Å on each atom in the equilibrium configuration of the system.

Considering that the construction of the sliding interlayer energy landscape is a computationally demanding task, we have chosen graphene as our model substrate system. Since the dominant interaction between the BN release layer and the graphene substrate is governed by the relatively weak vdW interaction, we expect the BN/graphene interface would provide a lower limit to the sliding barrier for a given device.¹² In other words, if the generic sapphire substrate is used, the sliding barrier is expected to be significantly higher than that calculated for the graphene substrate due to the higher polarity of the sapphire substrate.

The interfaces were modeled by GaN/BN, BN/graphene, and BN/BN bilayers, knowing that the *h*-BN release layer is usually of several nm thickness.⁶ We also assume that the atoms at the interface are free to relax in each of the bilayer. Therefore, one may see a variation in the B–N bond length at the two hetero-interfaces and through the BN layer. Considering the relatively large lattice mismatch in the in-plane lattice constants of GaN (~3.3 Å) and BN (~2.5 Å), we have explored two cases: (1) a 1:1 GaN to BN lattice ratio; (2) a commensurate $2 \times 2 \mathbf{R}$ GaN/ $\sqrt{7} \times \sqrt{7} \mathbf{R}$ BN

^{a)}Electronic mail: sims@lzu.edu.cn

^{b)}Electronic mail: haiying.he@valpo.edu

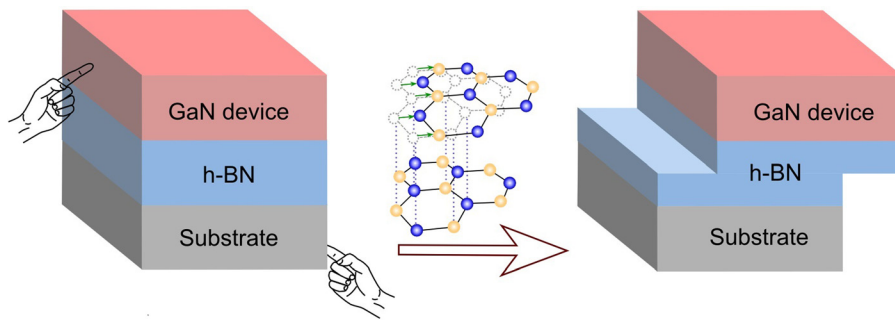


FIG. 1. A schematic diagram showing that a GaN-based device can be transferred from one substrate to another through the *h*-BN release layer.

supercell (Fig. 2(a)). In the latter case, the lattice mismatch is reduced to $\sim 3\%$. Initially, a full optimization of the in-plane configurations of the GaN/BN and BN/graphene bilayers was performed for different stacking configurations with an intention to locate the lowest energy stacking configuration. And it was followed by calculating the potential energy surface while varying the interlayer separation d (Fig. 3), thereby the equilibrium interlayer distance for the bilayer system was obtained. Note that the latter calculations were performed for the energetically preferred stacking configurations, which are AA' (e.g., inset of Fig. 4(c)) for GaN/BN at the 1:1 lattice matched conditions and AB_B (e.g., inset of Fig. 4(d)) for BN/graphene.^{13,14} However, for the GaN/BN unstrained bilayer, there is no such ideally stacked structure. Some B atoms (or N atoms) belonging to BN will always be on top of Ga atoms (or N atoms) of the GaN layer, and the repelling between these atoms results in weaker interlayer interaction and larger interlayer distance. Both the revPBE and vdW + PBE calculations yield the in-plane BN lattice constants of 2.91, 2.51, and 2.51 Å for GaN/BN case (1), GaN/BN case (2), and BN/graphene bilayers, respectively. While the BN layer remains a planar configuration, the GaN layer is buckled with an out-of-plane distance of 0.50 Å for the case (1). On the other hand, the GaN layer is relaxed into a planar structure for the unstrained GaN/BN case (2). The adhesion energy in the asymptotic limit, i.e., the difference in total energy at a separation d and at a separation large enough to eliminate inter-layer interaction, is

calculated as shown in Figure 3. For GaN/BN case (1), (2), and BN/graphene, the revPBE values for the equilibrium interlayer distance are 4.20, 4.57, and 4.25 Å, respectively. On the other hand, the vdW + PBE values for the equilibrium interlayer distance are 2.99, 3.62, and 3.39 Å for GaN/BN case (1), (2) and BN/graphene, respectively. It turns out that the vdW interaction plays an important role in determining the interlayer distance of two-dimensional materials.^{13,14} The revPBE exchange and correlational functional form of DFT appears to overestimate the interlayer distance of the considered bilayers.

The transfer process is now investigated by mapping out the sliding energy landscape constraining the layers to be at the equilibrium configuration. In order to further validate our approach, we first calculated BN/BN bilayer which was studied previously.^{7,8} Our calculated energy barrier of 2.0 meV/atom¹⁵ compares well with the previously reported values of 0.5 and 3.4 meV/atom for the case of the BN/BN system.^{7,8}

Figures 4(a) and 4(b) display the energy landscape during the sliding processes of the GaN/BN case (1) and BN/graphene bilayers, respectively, both with a 1:1 lattice matched condition. For GaN/BN case (1), the energetically preferred stacking order is AA' (Fig. 4(c)). Similar to the case of the BN/BN, the energy landscape of GaN/BN case (1) exhibits a sliding path with a minimum energy barrier [shown by the arrow in Fig. 4(a)]. Fig. 4(c) shows that the minimum energy barrier of 4.5 meV/atom is required to separate GaN/BN. This barrier is more than double of the value required for BN/BN.

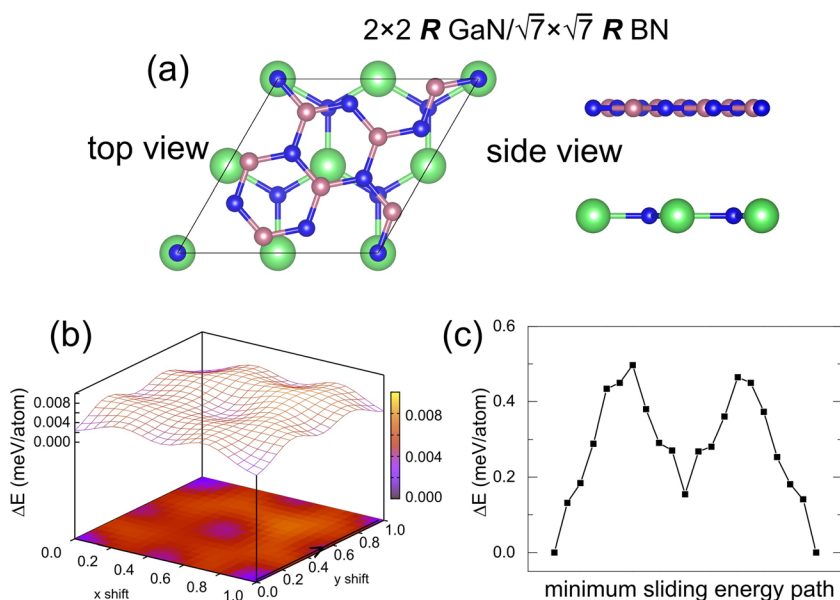


FIG. 2. Simulation of the unstrained GaN/BN bilayer with (a) the structure of $2 \times 2 \mathbf{R} \text{ GaN}/\sqrt{7} \times \sqrt{7} \mathbf{R} \text{ BN}$ supercell, (b) the corresponding sliding energy surface, and (c) the energy barrier along the path as illustrated in (b).

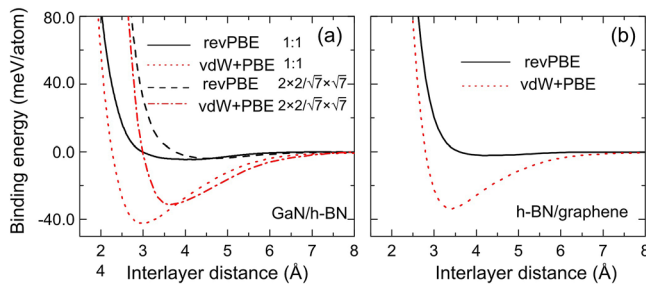


FIG. 3. Binding energy of (a) GaN/BN and (b) BN/graphene bilayers as a function of the interlayer distance calculated at the revPBE and vdW + PBE levels of theory. The GaN/BN bilayer maintains a AA' stacking at a 1:1 GaN to BN lattice ratio, while shows a mixed stacking at a commensurate $2 \times 2 \sqrt{7} \times \sqrt{7}$ GaN/ $\sqrt{7} \times \sqrt{7}$ BN lattice match. The BN/graphene bilayer favors AB_B stacking.

Thus, compared with GaN/BN, the sliding separation is easier to occur within the BN/BN bilayer. On the other hand, the calculated energy landscape in BN/graphene exhibits distinctly different features as compared with the BN/BN and GaN/BN [Fig. 4(b)]. An energy barrier plateau exists along the path [Fig. 4(d)] with the barrier of 3.8 meV/atom. The calculated results therefore imply that the sliding in BN/graphene is stiffer compared with the case of the BN bilayer. Considering that our focus in this study is on the relative energy variation along the sliding path, difference of a few tens of meV gives reliable differentiation in their energy, despite the fact that

accuracy of DFT calculations is usually beyond that. This point is further verified by the consistency in the calculated results indicating that they are “signals” rather than “noise”. And energy variations around similar order of magnitude obtained using density functional method were previously reported.⁷

It is, however, noteworthy to see the difference in the results for the GaN/BN case (2) with the unstrained interface. As discussed above (Fig. 3(a)), the interlayer distance increases from 2.99 to 3.62 Å going from the strained structure of case (1) to the unstrained structure of case (2). And the adhesion energy at the interface decreases from 42.6 (of case (1)) to 31.6 meV/atom (of case (2)). Furthermore, interactions in case (2) appear to be mainly governed by vdW interactions. As a result, the sliding barrier of this unstrained interface is extremely small (0.5 meV/atom), as shown in the sliding energy surface (Fig. 2(c)). The calculated results therefore suggest that the unstrained GaN is easy to peel off from the BN layer. It also explains the experimental observation that high-quality nitride semiconductors could only be grown on *h*-BN with an AlN or AlGaIn buffer layer.⁶ Such a buffer layer could lead to a better lattice match between dissimilar materials and enforces the electrostatic interactions, thereby increases the sliding barrier to help with the adhesion between GaN and BN. Further studies of buffer-layer/GaN and buffer-layer/BN interfaces are needed to provide a quantitative description of the barrier.

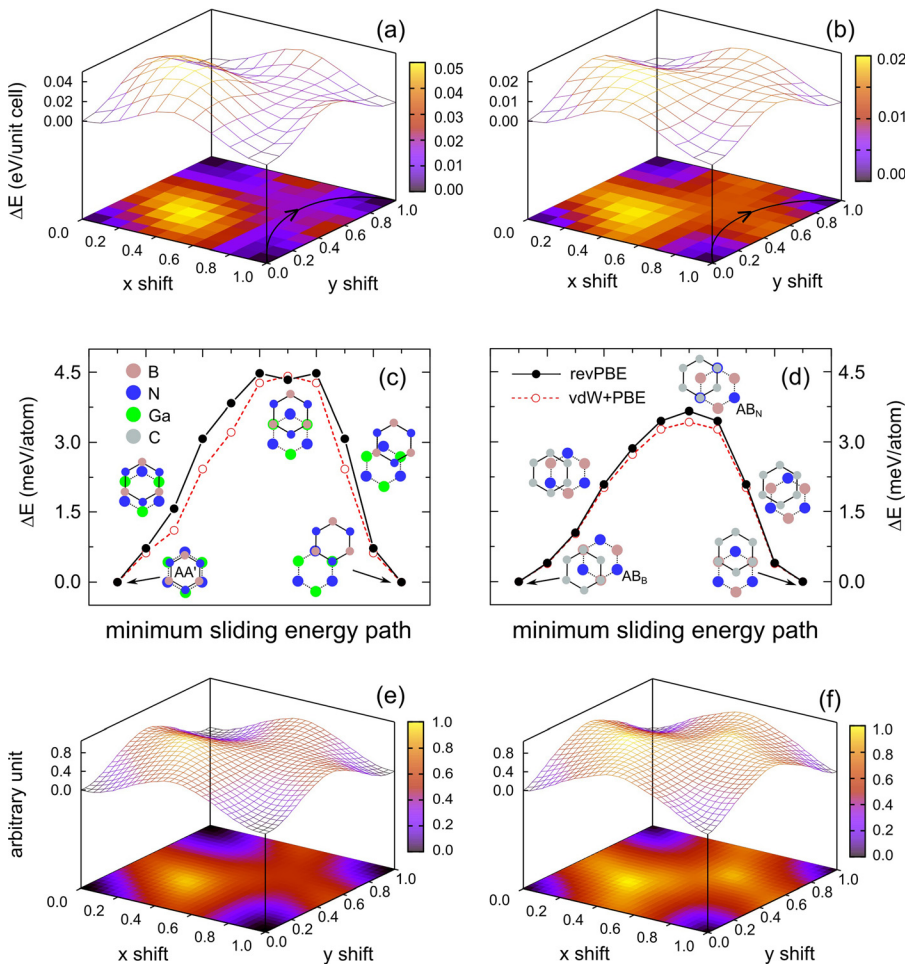


FIG. 4. The energy landscapes for the (a) GaN/BN (strained) and (b) BN/graphene systems. The lowest-energy sliding paths for the (c) GaN/BN (strained) and (d) BN/graphene systems. Both revPBE (black solid symbol) and vdW + PBE (red empty symbol) results are presented. The calculated registry index surfaces for the (e) GaN/BN (strained) and (f) BN/graphene systems.

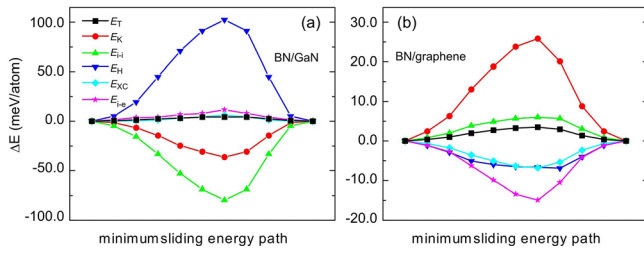


FIG. 5. Variation of the total (black square), kinetic (red circle), ion-ion Coulomb interaction (green up-triangle), Hartree (blue down-triangle), exchange-correlation (cyan diamond), and ion-electron Coulomb interaction (magenta star) DFT energy components along the lowest-energy sliding paths for (a) GaN/BN (strained) and (b) BN/graphene. Zero of the energy is defined as the value of the relevant component at the lowest-energy configuration.

To understand the underlying separation mechanism during the sliding process for the strained GaN/BN interface (case (1)), we directly compare the sliding energy landscapes calculated using the revPBE and vdW exchange and correlation functional forms. Their close similarity in the energy variation along the lowest energy sliding path suggests [Figs. 4(c) and 4(d)] that the sliding process is dominated by the interlayer electrostatic interactions, but not the vdW interaction which simply anchors the layers at an appropriate distance. This point is directly manifested by our finding that the binding energies obtained from the vdW calculations are significantly larger than those obtained from the revPBE calculations (see Fig. 3).

Decomposition of the total energy of the system (Fig. 5), however, reveals very different energy dependence for GaN/BN and BN/graphene. In the case of GaN/BN, the Hartree energy varies by 102.5 meV/atom, along the minimum sliding energy path with its maximum at the same location as the maximum total energy. This change in the Hartree energy is largely offset by the change in kinetic energy and ion-ion Coulomb interaction terms. The change of the order of -80.0 meV/atom in the ion-ion Coulomb interaction term is due to higher ionicity of GaN relative to that of BN. Both ion-electron Coulomb interaction and exchange-correlation energy terms vary by a much smaller degree along the sliding path.

The BN/graphene bilayer shows a much different scenario with much smaller variations in its Hartree energy and ion-ion Coulomb interaction terms owing to the homonuclear bonds in graphene. The maximum variation in kinetic, ion-electron interaction and exchange-correlation energy is

about the same as calculated for GaN/BN. In addition, it is interesting to observe that the sign of the energy variation along the minimum sliding energy path in all its energy components are reversed as compared to the case of GaN/BN.

The distinctly different behavior of GaN/BN and BN/graphene systems is also visible in their charge distributions. Figure 6 displays the deformation charge densities (i.e., charge density of the system with reference to the sum of the charge densities of its constituent atoms) at the minimum energy and barrier-energy configurations. Graphene shows a typical sp^2 hybridization with C-C covalent bonds (i.e., excess electrons over C-C bonds); while semi-ionic GaN is featured by near-spherical electron-excess and electron-deficient regions centered on N and Ga ions of the system. The BN layer in both GaN/BN and BN/graphene bilayers, however, show similar trigonal electron-deficient regions around the B atoms and the electron-excess regions near N atoms and along N-B bonds due to the relatively weak interlayer interactions.

One can therefore conclude that (i) the minimum energy configuration is associated with a stacking when the electron-excess and electron-deficient regions from those two layers compensate to each other minimizing the electrostatic interactions. On the contrary, the barrier-energy configuration is associated with a stacking with the larger Coulomb repulsion between like charges of the two layers along the sliding pathway; (ii) there is no visible change in the deformation charge densities in individual layers either at the minimum energy configuration or at the barrier-energy configuration along the sliding pathway. In other words, two layers shift against each other as if rigid planes with barely disturbed charge distributions. The sliding barrier is then predominantly determined by the electrostatic interaction energy between the constituent layers.

These observations then lead us to consider the registry index (RI) model first proposed by Hod,^{16,17} among other microscopic mechanisms of the interlayer sliding process in layered materials.^{17–20} The RI model has been successfully applied to predict the interlayer sliding energies for homogeneous layer structures such as planar hexagonal boron-nitride, graphitic systems, and multi-layered nanotubes. By using simple geometric considerations, the RI model is able to capture the complex physical features of interlayer sliding in layered materials with the modest computational resources.

Due to the polar nature of B-N and Ga-N bonds, the RI for GaN/BN is defined as

$$RI_{\text{GaN/h-BN}} = \frac{(S_{NN} - S_{NN}^{AA'}) + (S_{BGa} - S_{BGa}^{AA'}) - (S_{NGa} - S_{NGa}^{AA'}) - (S_{BN} - S_{BN}^{AA'})}{(S_{NN}^{AA} - S_{NN}^{AA'}) + (S_{BGa}^{AA} - S_{BGa}^{AA'}) - (S_{NGa}^{AA} - S_{NGa}^{AA'}) - (S_{BN}^{AA} - S_{BN}^{AA'})}, \quad (1)$$

where S_{ij} represents the overlap of the centered circles between the top i and the bottom j atoms. The superscripts AA and AA' denote the two reference stacking configurations.

As the normalized denominator is used in Eq. (1), a value of $RI = 1$ is associated with the least favorable stack arrangement, while the value of $RI = 0$ indicates the energetically

preferred configuration. The RI as a function of lateral shift can be obtained by using the radii of N (r_N), B (r_B), and Ga (r_{Ga}) atoms as the fitting parameters. For simplicity, we assume that the N atoms in BN and GaN hold the same radius r_N .

A good agreement between RI surface and the energy landscape is then obtained based on the parameters

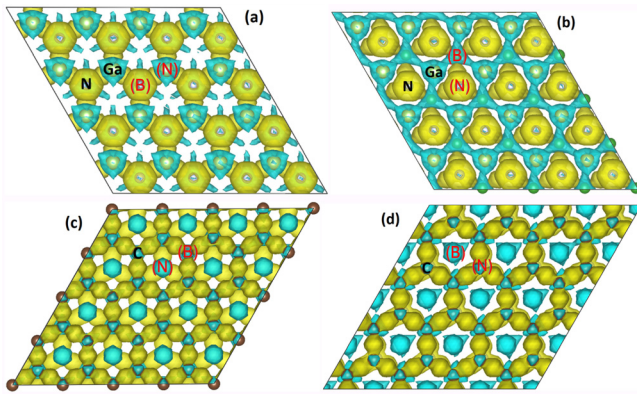


FIG. 6. Deformation charge density plots (top view) for the lowest-energy configurations of (a) GaN/BN (strained) and (c) BN/graphene; and for the barrier-energy configurations of (b) GaN/BN (strained) and (d) BN/graphene. GaN or graphene is shown on the top with black atomic labels, while the bottom BN layer is labeled in red with brackets. The isosurface value is set to be 1/6 of the maximum charge density for each case with a specific value of $0.007 \text{ e}/\text{\AA}^3$ and $0.011 \text{ e}/\text{\AA}^3$ for GaN/BN and BN/graphene, respectively.

$r_N = 0.727 \text{ \AA}$, $r_B = 0.253 \text{ \AA}$, and $r_{\text{Ga}} = 0.872 \text{ \AA}$. The RI surface, as shown in Fig. 4(e), resembles the quantum mechanical potential energy surface shown in Fig. 4(a). Although the N atoms possess nearly the same radii in this model, a large disparity in radii appears between the B and Ga atoms inducing a strong polarization of atoms along the vertical direction.²¹ And the interlayer electrostatic interactions are enhanced via the strong polarized atoms or the electric dipole interactions. Thus, a high energy barrier to slide GaN/BN comes out to be a natural consequence of physics and chemistry of the system.

The case of BN/graphene is slightly different compared with the other two cases as graphene is an identical π polar system to BN. The corresponding RI is defined as

$$RI_{h\text{-BN/graphene}} = \frac{(S_{CN} - S_{CN}^{AB_B}) + (S_{CB} - S_{CB}^{AB_B})}{(S_{CN}^{AA} - S_{CN}^{AB_B}) + (S_{CB}^{AA} - S_{CB}^{AB_B})}, \quad (2)$$

where superscripts AA and AB_B are referred to the two configurations [Fig. 4(d)].

The RI surface of BN/graphene is simulated with parameters $r_N = 0.727 \text{ \AA}$, $r_C = 0.752 \text{ \AA}$, and $r_B = 0.218 \text{ \AA}$. A good agreement between Figs. 4(f) and 4(b) indicates that the energy landscape can be reproduced by the RI surface. Similarly, a large disparity in radii between the B and C atoms justify the requirement of a relatively large barrier to separate the BN/graphene system.

In summary, we have carried out calculations based on density functional theory to demonstrate why the transfer of GaN/BN/substrate can be achieved through the *h*-BN release layer. Comparison of the interlayer sliding energy landscapes finds that a nearly free sliding path not only occurs within

BN/BN but also for the strained GaN/BN and BN/graphene. The calculated energy barrier of about 4.5 meV/atom is required to separate the strained GaN/BN bilayer with the substrate being graphene at a 1:1 lattice matched condition. It is much larger than the calculated barrier of 2.0 meV/atom for the case of BN/BN. Although the vdW interaction term determines the equilibrium interlayer distance for the considered system, the interlayer sliding process relies critically on the electrostatic interactions between the constituent layers of the system. We show that this effect can also be captured by a simple phenomenological model—the registry index model. The unstrained GaN/BN interface of case (2), however, appears to have small adhesion energy indicating the requirement for a buffer layer in the growth of single crystal GaN on BN.

This work was supported by the National Basic Research Program of China under No. 2012CB933101 and the Fundamental Research Funds for the Central Universities (No. 2022013zrct01). This work was also supported by the National Science Foundation of China (Nos. 51202099 and 51372107). The MTU Superior supercomputing facility is acknowledged.

¹H. Amano, M. Kito, K. Hiramatsu, and I. Akasaki, *Jpn. J. Appl. Phys., Part II* **28**, L2112 (1989).

²D. P. Bour, N. M. Nickel, C. G. Van de Walle, M. S. Kneissl, B. S. Krusor, P. Mei, and N. M. Johnson, *Appl. Phys. Lett.* **76**, 2182 (2000).

³J. L. Lyons, A. Janotti, and C. G. Van de Walle, *Phys. Rev. Lett.* **108**, 156403 (2012).

⁴D. I. Florescu, V. M. Asnin, and F. H. Pollak, *Appl. Phys. Lett.* **77**, 1464 (2000).

⁵W. S. Wong, T. Sands, and N. W. Cheung, *Appl. Phys. Lett.* **72**, 599 (1998).

⁶Y. Kobayashi, K. Kumakura, T. Akasaka, and T. Makimoto, *Nature* **484**, 223 (2012).

⁷N. Marom, J. Bernstein, J. Garef, A. Tkatchenko, E. Joselevich, L. Kronik, and O. Hod, *Phys. Rev. Lett.* **105**, 046801 (2010).

⁸G. Constantinescu, A. Kuc, and T. Heine, *Phys. Rev. Lett.* **111**, 036104 (2013).

⁹Y. Zhang and W. Yang, *Phys. Rev. Lett.* **80**, 890 (1998).

¹⁰G. Roman-Perez and J. M. Soler, *Phys. Rev. Lett.* **103**, 096102 (2009).

¹¹D. Sánchez-Portal, P. Orderjón, E. Artacho, and J. M. Soler, *Int. J. Quantum Chem.* **65**, 453 (1997).

¹²A. K. Geim and I. V. Grigorieva, *Nature* **499**, 419 (2013).

¹³X. Zhong, Y. K. Yap, R. Pandey, and S. P. Karna, *Phys. Rev. B* **83**, 193403 (2011).

¹⁴D. Xu, H. He, R. Pandey, and S. P. Karna, *J. Phys.: Condens. Matter* **25**, 345302 (2013).

¹⁵See supplementary material at <http://dx.doi.org/10.1063/1.4896506> for the sliding energy barrier of the BN bilayer.

¹⁶O. Hod, *Isr. J. Chem.* **50**, 506 (2010).

¹⁷O. Hod, *Phys. Rev. B* **86**, 075444 (2012).

¹⁸A. E. Filippov, M. Dienwiebel, J. W. M. Frenken, J. Klafter, and M. Urbakh, *Phys. Rev. Lett.* **100**, 046102 (2008).

¹⁹W. Zhong and D. Tomanek, *Phys. Rev. Lett.* **64**, 3054 (1990).

²⁰S. Cahangirov, C. Ataca, M. Topsakal, H. Sahin, and S. Ciraci, *Phys. Rev. Lett.* **108**, 126103 (2012).

²¹F. D. Sala, S. Blumstengel, and F. Henneberger, *Phys. Rev. Lett.* **107**, 146401 (2011).